Bitlis Eren Üniversitesi Fen Bilimleri Dergisi
BİTLİS EREN UNIVERSITY JOURNAL OF SCIENCE
ISSN: 2147-3129/e-ISSN: 2147-3188
VOLUME: 12 NO: 4 PAGE: 1171-1184 YEAR: 2023
DOI:10.17798/bitlisfen.1358965

Evaluation of Road Roughness and Vehicle Speed Effects on Vibration Comfort of School Bus Driver Seats following the ISO 2631-1 Standard and Occupational Health and Safety Legislation

Akif YAVUZ[1], Suleyman Enes HACIBEKTASOGLU[2*]

[1]*Istanbul Technical University Department of Mechanical Engineering, Istanbul, Türkiye*
[2]*Sinop University Department of Occupational Health and Safety, Sinop, Türkiye*
(ORCID: 0000-0002-9447-7306) (ORCID: 0000-0002-8997-8480)

Keywords: School bus driver, Vehicle seat comfort, Road roughness, Seat vibrations, Occupational health and safety

Abstract
Human perception in terms of vehicle comfort problems is a significant issue for automotive manufacturers and academic researchers, as evident from the scientific papers available in the literature. In this study, the maximum vehicle speed is predicted for the comfortable driving of school bus drivers under certain working conditions. First, a full-vehicle school bus model, which consists of a seat, vehicle body, wheels, and suspension systems, is developed to evaluate vehicle seat comfort following ISO 2631-1 and Occupational Health and Safety (OHS) legislation. Second, the experimentally collected power spectrum densities of road roughness are converted to amplitude form in order to be an input to the developed full-vehicle model. Third, the frequency weighting factor, which is determined by ISO 2631-1, is applied to the calculated RMS acceleration of the seat. Finally, frequency-weighted RMS accelerations of the seat for various conditions of road roughness and vehicle speeds are obtained, and they are used to evaluate the bus driver seat comfort by ISO 2631-1. In addition, RMS accelerations of the bus driver seat are used to evaluate vehicle seat comfort by OHS legislation. It is concluded that the effects of vehicle speed and road roughness on comfortable driving are observed, and maximum vehicle speed for comfortable driving decreases as the power spectrum density of road roughness increases. According to the results, measures to be taken following the OHS legislation are suggested.

1. Introduction

Vibration-induced vehicle problems are a considerably significant issue regarding human health and comfort. Nowadays, many automotive companies aim to minimize tiredness and discomfort during long journeys due to vehicle seat vibrations. Therefore, studies in the literature about vehicle comfort problems have investigated that vehicle seat vibrations in the normal direction cause health problems for drivers and passengers. Long-duration and high-amplitude vibrations have physiological and psychological problems for humans, such as motion sickness and discomfort. Many automotive manufacturers and academic researchers have been working for a long time to reduce the amplitude of seat vibrations [1]-[3].

With the OHS activities carried out in the workplace, employers aim to ensure that the employees are in a state of complete physical and mental well-being. In this context, it is necessary to determine the hazards in the working environment and the risks arising from these hazards. Employers are obliged to take measures to eliminate these determined risks or to bring them to an acceptable level in accordance with the OHS regulations. For this purpose, the risk assessment studies to be carried out in the workplaces should be applied in detail with a risk analysis method that is suitable for the workplace, and the precautions to be taken should be determined [4]-[7].

*Corresponding author: *shacibektasoglu@sinop.edu.tr*
Received: 12.09.2023, Accepted: 11.12.2023

Vibration is one of the physical risk factors that employees are exposed to due to the machinery and equipment they use in the workplace. Based on the type of work, they are exposed to hand-arm or whole-body vibration. As a result of this exposure, employees experience various health problems, especially in the musculoskeletal system. In Türkiye, in accordance with the Occupational Health and Safety Law No. 6331, which was enacted in 2012, employers are obliged to carry out risk assessments to ensure the safety and health of employees at workplaces. In addition, according to the regulation of vibration enacted in accordance with this law, the limit values to which employees can be exposed to different types of vibration are given in Table 1. Vibration exposure values should be determined with the measurements, and these values should be reduced to an acceptable level with the precautions for inappropriate values [8]-[12].

Table 1. Exposure values for exposure types in accordance with OHS regulations [8]

Types of Exposure	**Exposure Action Value (m/s^2)**	**Exposure Limit Value (m/s^2)**
Hand-Arm Vibration	2,5	5
Whole Body Vibration	0,5	1,15

The oscillations on the vehicle body due to road excitations are generally between the frequencies of 0 Hz and 25 Hz [13]. The road roughness, which is an input of vehicle system dynamics, is transferred to the wheel, and then it is transmitted to the axle body with the elastic parts of the vehicle [14]. Synthetic road profiles, depending on ISO 8608 classifications, are commonly used for simulating various tasks in vibration analysis. Múčka's study compared these synthetic road classes with real road spectra and found significant differences [15]. There are also many studies in the field of road surface [16]-[18]. In addition to the road roughness, driving characteristics and the transmission path of vibration, which is a characteristic for transferring vibration signals from road excitation to the seat, cause discomfort while driving. Vehicle comfort, corresponding to seat vibrations in the vertical direction, is a significant parameter that affects the driver's health. In order to evaluate the vehicle's comfort related to the driver seat, rms vertical acceleration data in the time domain of the driver seat is used as an identification parameter of comfort [19]. The effects of vertical seat acceleration amplitudes on comfortable driving were investigated by an analytical model of the selected vehicle [20]. To evaluate the vehicle comfort, in addition to the acceleration data from the seat, International Standardization Organization (ISO) 2631-1 is also implemented. ISO 2631-1 was developed under the purview of the Technical Committee ISO/TC 108, which is responsible for matters related to mechanical vibration and shock. The principal objective of ISO 2631-1 is to delineate quantitative methodologies pertaining to whole-body vibration, encompassing aspects related to human health, comfort, the discernibility of vibration, as well as the potential effects of vibration on the occurrence of health-related issues, as referenced in [21]. Using ISO 2631-1 to evaluate the comfort of a vehicle seat in the vertical direction is a widely performed method in terms of vibration data. The criteria of rms acceleration and frequency-weighted transformations in ISO 2631-1 are considered a method of vehicle comfort evaluation.

In this study, a full vehicle vibration model, which has eight degrees of freedom, is developed to investigate the effect of vehicle speed and road roughness on comfortable driving in accordance with ISO 2631-1 and OHS legislation. The eight-degrees–of-freedom model consists of a linear elastic spring and damping elements. Note that the input of the mathematical model is the road excitations, which are obtained experimentally for different types of roads. The linear equations of motion are solved with the Runge-Kutta time step integration to obtain time-series responses such as the RMS acceleration data of the bus driver seat. Thus, the frequency-weighted RMS acceleration data of the bus driver seat is determined by the frequency-weighted curve in ISO 2631-1 to evaluate vehicle comfort. Consequently, the main objectives of this study are listed as follows: 1) Evaluation of road roughness and vehicle speed effects on the vibration comfort of the school bus driver seat using frequency-weighted RMS accelerations of the seat in conjunction with ISO 2631-1 2) Determine the maximum vehicle speed for comfortable driving of different types of roads, which are concrete, asphalt, cobblestone, and dirt, in accordance with ISO 2631-1 3) Evaluation of road roughness and vehicle speed effects on the vibration comfort of the school bus driver seat using RMS accelerations of the seat in accordance with OHS legislation 4) Comparison of ISO 2631-1 evaluations and OHS legislation evaluations in terms of school bus driver seat comfort. The main purpose of the study is to compare the OHS regulations in Türkiye with ISO 2631 in terms of whole-body vibrations. When both regulations are compared, it is observed that ISO 2631-1 is more comprehensive and categorizes exposure. The novelty of this study is to detect the performance of whole-body vibration assessments with OHS legislation from Türkiye compared to ISO 2631-1.

2. Mathematical Model School Bus

The full-vehicle model, which consists of mass-spring-damping elements, is developed to mimic a real vehicle in terms of the dynamic behaviors of a vehicle. The comprehensive full-vehicle analytical model is visually represented in Figure 1, while the corresponding definitions and symbols employed in the model can be found in Table 2. The developed full-vehicle model with a passive suspension system has pitch and roll motion at the body. The eight degrees of freedom model has a vertical motion of the seat, body, and four wheels, and two rotational motions of the body. The rolling and pitch angles of the body are assumed to be very small to simplify the system in accordance with real vehicle dynamics. Vehicle suspension systems in the model are assumed to be linear and passive. The tires within the vehicle system are conceptualized as linear springs devoid of dampening mechanisms. The formulation of the differential equations governing motion is dependent on Newton's second law, which is facilitated through the utilization of the free-body diagram framework. These equations are represented as Equations 1-8.

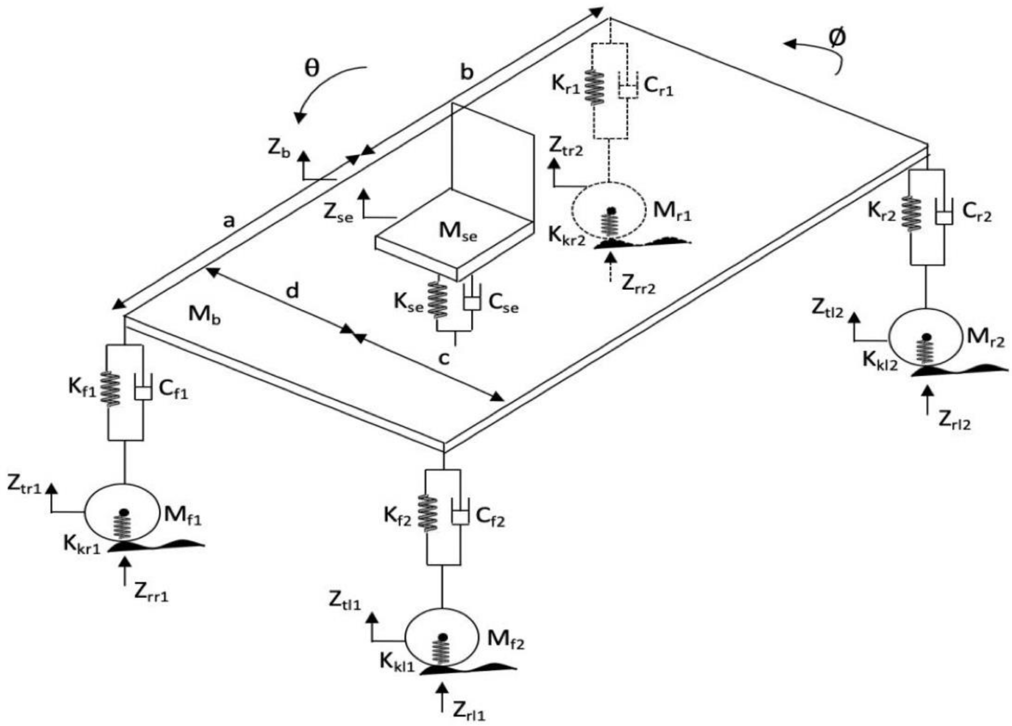

Figure 1. Full vehicle model of school bus.

Table 2. Definitions and symbols of the full-vehicle model.

C_{se}	seat damping coefficient	M_{f1}	front right wheel unsprung mass
C_{f1}	front right suspension damping	M_{f2}	front left unsprung wheel mass
C_{f2}	front left suspension damping	M_{r1}	rear right wheel unsprung mass
C_{r1}	rear right suspension damping	M_{r2}	rear left wheel unsprung mass
C_{r2}	rear left suspension damping	Z_{rr1}	front right road roughness
K_{se}	seat stiffness	Z_{rl1}	front left road roughness
K_{f1}	front right suspension stiffness	Z_{rr2}	rear right road roughness
K_{f2}	front left suspension stiffness	Z_{rl2}	rear left road roughness

K_{r1}	rear right suspension stiffness	Z_b	vehicle body vertical displacement
K_{r2}	rear left suspension stiffness	Z_{se}	seat vertical displacement
K_{kr1}	front right tire stiffness	Z_{tr1}	front right wheel vertical displacement
K_{kl1}	front left tire stiffness	Z_{tl1}	front left wheel vertical displacement
K_{kr2}	rear right tire stiffness	Z_{rr2}	rear right wheel vertical displacement
K_{kl2}	rear left tire stiffness	Z_{rl2}	rear left wheel vertical displacement
M_b	vehicle body mass	θ	pitch angle of vehicle body
M_{se}	seat mass	$\emptyset$	roll angle of vehicle body
a	distance from the sprung vehicle body mass CG to the front axle	b	distance from the sprung vehicle mass CG to the rear axle
c	distance from the sprung vehicle body mass CG to the vehicle left side	d	distance from the sprung vehicle mass CG to the vehicle right side

$$M_b\ddot{Z}_b + Z_b(K_{f1} + K_{f2} + K_{r1} + K_{r2}) + (C_{f1} + C_{f2} + C_{r1} + C_{r2})\dot{Z}_b - (K_{f1}a + K_{f2}a - K_{r1}b - K_{r2}b)\theta - (C_{f1}a + C_{f2}a - C_{r1}b + C_{sl2}b)\dot{\theta} - (K_{f1}c - K_{f2}d - K_{r1}c + K_{r2}d)\emptyset - (C_{f1}c - C_{f2}d + C_{r1}c - C_{r2}d)\dot{\emptyset} + K_{se}(Z_b - Z_{se} + \theta c - \emptyset a) + C_{se}(\dot{Z}_b - \dot{Z}_{se} + \dot{\theta}c - \dot{\emptyset}a) - K_{f1}Z_{wr1} - K_{f2}Z_{tl1} - K_{r1}Z_{tr2} - K_{r2}Z_{tl2} - C_{f1}\dot{Z}_{tr1} - C_{f2}\dot{Z}_{tl1} - C_{r1}\dot{Z}_{tr2} - C_{r2}\dot{Z}_{tl2} = 0 \quad (1)$$

$$I_{yy}\ddot{\theta} - K_{f1}(Z_b - \theta a - \emptyset c + Z_{tr1})a - K_{f2}(Z_b - \theta a + \emptyset d - Z_{tl1})a + K_{r1}(Z_b + \theta b - \emptyset c - Z_{tr2})b + K_{r2}(Z_b + \theta b + \emptyset d - Z_{tl2})b + C_{f1}(\dot{Z}_b - \dot{\theta}a - \dot{\emptyset}c - \dot{Z}_{tr1})a - C_{f2}(\dot{Z}_b - \dot{\theta}a + \dot{\emptyset}d - \dot{Z}_{tl1})a + C_{r1}(\dot{Z}_b + \dot{\theta}b - \dot{\emptyset}c - \dot{Z}_{tr2}) + C_{r2}(\dot{Z}_b + \dot{\theta}b + \dot{\emptyset}d - \dot{Z}_{tl2})b + K_{se}(Z_b - Z_{se} + \theta c - \emptyset a) + C_{se}(\dot{Z}_b - \dot{Z}_{se} + \dot{\theta}c - \dot{\emptyset}a) = 0 \quad (2)$$

$$I_{xx}\ddot{\emptyset} - -K_{f1}(Z_b - \theta a - \emptyset c + Z_{tr1})c + K_{f2}(Z_b - \theta a + \emptyset d - Z_{tl1})d - K_{r1}(Z_b + \theta b - \emptyset c - Z_{tr2})c + K_{r2}(Z_b + \theta b + \emptyset d - Z_{tl2})d - C_{f1}(\dot{Z}_b - \dot{\theta}a - \dot{\emptyset}c - \dot{Z}_{tr1})c + C_{f2}(\dot{Z}_b - \dot{\theta}a + \dot{\emptyset}d - \dot{Z}_{tl1})d - C_{r1}(\dot{Z}_b + \dot{\theta}b - \dot{\emptyset}c - Z_{tr2})c + C_{r2}(\dot{Z}_b + \dot{\theta}b + \dot{\emptyset}d - \dot{Z}_{tl2})d - K_{se}(Z_b - Z_{se} + \theta c - \emptyset a) - C_{se}(\dot{Z}_b - \dot{Z}_{se} + \dot{\theta}c - \dot{\emptyset}a) = 0 \quad (3)$$

$$M_{f1}\ddot{Z}_{wr1} - K_{f1}(Z_b - \theta a - \emptyset c - Z_{tr1}) + K_{kr1}(Z_{tr1} - Z_{rr1}) - C_{f1}(\dot{Z}_b - \dot{\theta}a - \dot{\emptyset}c - \dot{Z}_{wr1}) = 0 \quad (4)$$

$$M_{f2}\ddot{Z}_{wl1} - K_{f2}(Z_b - \theta a - \emptyset c - Z_{tl1}) + K_{kl1}(Z_{tl1} - Z_{rl1}) - C_{f2}(\dot{Z}_b - \dot{Z}_{tl1} - \dot{\theta}a - \dot{\emptyset}c) = 0 \quad (5)$$

$$M_{r1}\ddot{Z}_{wr2} - K_{r1}(Z_b - \emptyset c - Z_{tr2} - \theta a) + K_{kr2}(Z_{tr2} - Z_{rr2}) - C_{r1}(\dot{Z}_b - -\dot{Z}_{tr2} - \dot{\theta}a - \dot{\emptyset}c) = 0 \quad (6)$$

$$M_{r2}\ddot{Z}_{wl2} - K_{r2}(Z_b - Z_{tl2} - \theta a - \emptyset c) + K_{kl2}(Z_{tl2} - Z_{rl2}) - C_{r2}(\dot{Z}_b - \dot{\emptyset}c - \dot{\theta}a - \dot{Z}_{tl2}) = 0 \quad (7)$$

$$M_{se}\ddot{Z}_{se} - K_{se}(\theta c + Z_b - Z_{se} - \emptyset a) - C_{se}(\dot{\theta}c + \dot{Z}_b - \dot{Z}_{se} - \dot{\emptyset}a) = 0 \quad (8)$$

Road roughness for the different classes of roads, which are concrete, asphalt, cobblestone, and dirt, is collected experimentally in terms of displacement power spectrum density ($\Phi_h(\Omega_0)[cm^3]$). In order to be the input parameter for road excitation in the developed full-vehicle model, the obtained road roughness should be determined as an amplitude instead of $\Phi_h(\Omega_0)$. Hence, experimentally measured power spectrum densities (PSD) based on reference angular spatial frequency ($\Omega_0 = 1\ rad/m$) are converted to amplitude. Therefore, the full vehicle model can be excited by the amplitude as an input, which depends on the wavelength of road roughness. The full-vehicle car model is stimulated by road amplitudes with the same signal on the left and right sides of the school bus ($Z_{rr1} = Z_{rl1} = Z_{rr2} = Z_{rl2}$).

The RMS of the excitation function (Δh) is established within the framework of a defined wavelength range (ΔL), resulting in the derivation of a singular harmonic function denoted as $\hat{b}_{abs}$ amplitude, representative of the average wavelength (L). The inclusion of a √2 factor is assumed for the purpose of converting the harmonic function, as indicated by previous references [22], [23].

$$\widetilde{\Delta h} = \sqrt{\int_{\bar{L}-\Delta L/2}^{\bar{L}+\Delta L/2} \Phi_h(L) dL} = \sqrt{\Phi_h(\bar{L})\Delta L} = \frac{\hat{b}_{abs}}{\sqrt{2}} \quad (9)$$

$$\hat{b}_{abs} = \sqrt{\frac{\Omega^2}{\pi} \Phi_h(\Omega_0)\Delta L} \quad (10)$$

According to the experimental results, the concrete, asphalt, cobblestone, and dirt classes of roads are categorized as 4, 3, 4, and 4 road types, respectively. The road classes and their road types are given in Table 3. The transformation of the obtained displacement power spectrum density ($\Phi_h(\Omega_0)[cm^3]$) to amplitude calculations is performed for concrete, asphalt, cobblestone, and dirt roads, as given in Table 3. Note that the classes of A, B, C, and D roads, which are used in this study as road excitations, are good concrete ($\Phi_h(\Omega_0) = 3\ cm^3$), very good asphalt ($\Phi_h(\Omega_0) = 8\ cm^3$), medium cobblestone ($\Phi_h(\Omega_0) = 27\ cm^3$) and bad dirt ($\Phi_h(\Omega_0) = 60\ cm^3$), respectively. These four classes of road types are assumed to be input for the full-vehicle model. The simulated road profile is depicted for only good concrete roads ($\Phi_h(\Omega_0) = 3\ cm^3$) in Figure 2.

The sensitivity of people to whole-body vibrations varies with frequency. Frequency weighting factors evaluate the effects of frequencies on people [22]. The frequency weighting factors are determined in ISO 2631-1. In this study, W_k frequency weighting curve for vertical whole-body vibrations is used. It is given in Figure 2. The mathematical representation of the RMS acceleration of the seat (a_{rms}) is given in the Equation 11:

$$a_{rms} = \left\{ \frac{1}{T} \int_0^T [a(t)]^2 dt \right\}^{\frac{1}{2}} \quad (11)$$

$a(t)$ - seat acceleration (m/s²)
T - duration of the measurement in seconds (s).

Table 3. Measured PSD for different types of roads [21].

Road Class	Road Type	w	$\Phi_h(\Omega_0) cm^3$
Concrete	Very good	2.29	0.6
	Good (A)	1.97	3
	Medium	1.97	8.7
	Bad	1.72	56
Asphalt	Very good (B)	2.20	8
	Good	2.18	11
	Medium	2.18	22
Cobblestone	Good	1.75	14
	Medium (C)	1.75	27
	Bad	1.81	36
	Very bad	1.81	323
Dirt	Good	2.25	32
	Medium	2.25	44
	Bad (D)	2.14	60
	Very bad	2.14	16300

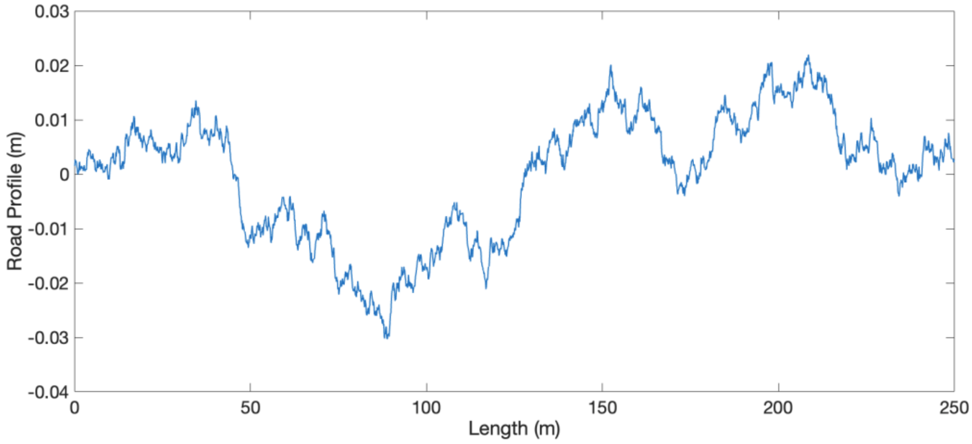

Figure 2. Road profile for good concrete.

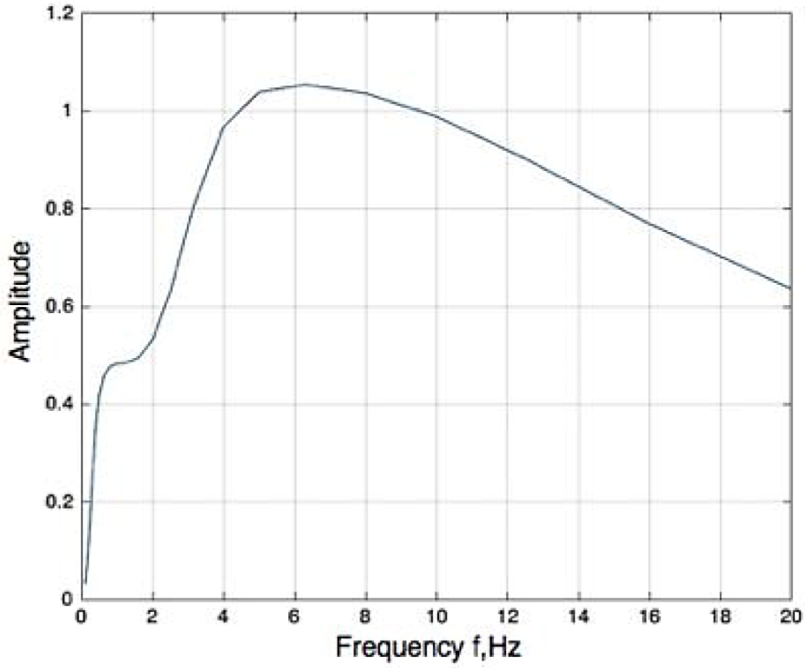

Figure 3. The converted $\mathbf{W_k}$ frequency weighting curve in ISO 2631-1 in terms of amplitude.

W_k frequency weighting curve is used to determine the frequency-weighted RMS accelerations of the seat in the vertical direction. The frequency-weighted acceleration (RMS) of the seat ($a_{w,rms}$) is obtained with the Equation 12:

$$a_{w,rms} = \left[\sum_i (W_i a_{rms})^2\right]^{\frac{1}{2}} \tag{12}$$

where $a_{w,rms}$ is the frequency-weighted RMS accelerations of the seat and W_i is the weighting factor.

3. Results

3.1. Evaluation with ISO 2631-1

To ascertain the RMS acceleration of the seat in the vertical direction, the governing linear equations are subject to numerical resolution through the utilization of the 4th-order explicit Runge-Kutta technique, thereby yielding temporal domain responses [24]. Furthermore, the calculated RMS acceleration of the seat from time series responses is converted to the frequency-weighted RMS accelerations of the seat in order to assess comfortable driving in accordance with ISO 2631-1. According to 2631-1, the seat frequency-weighted RMS acceleration of $\mathbf{0.315}\boldsymbol{m/s^2}$ value is the upper threshold for comfortable driving [22]. This threshold value of acceleration for comfortable driving is an assumed comfort criterion. Although this frequency-weighted RMS acceleration ($\mathbf{0.315}\boldsymbol{m/s^2}$) is the comfort limit value, the comfort zones corresponding to different frequency-weighted RMS acceleration values are classified in ISO 2631-1 (Table 4). When looking at the comfort zones, there are no exact sharp ranges; there are blurred ranges. However, the acceleration value evaluated in the study is assumed to be in the comfort range, where it is closer to the upper value. For example, the value of $\mathbf{0.55}\,\boldsymbol{m/s^2}$ is considered to be in the fairly uncomfortable zone, not a little uncomfortable zone. Because the lower initial value of the fairly uncomfortable zone ($\mathbf{0.5}\,\boldsymbol{m/s^2}$) is closer to $\mathbf{0.55}$.

Table 4. Comfort zones from ISO 2631-1.

Frequency-weighted RMS acceleration (m/s^2)	**Comfort Index**
$< \mathbf{0.315}$	Not uncomfortable
$\mathbf{0.315 - 0.63}$	A little uncomfortable
$\mathbf{0.5 - 1}$	Fairly uncomfortable
$\mathbf{0.8 - 1.6}$	Uncomfortable
$\mathbf{1.25 - 2.5}$	Very uncomfortable
$> \mathbf{2}$	Extremely uncomfortable

In order to understand the effects of road roughness and vehicle speed on comfortable driving, the full-vehicle model is analyzed at four different PSDs of road roughness. Frequency-weighted RMS accelerations of the bus seat in the vertical direction are determined for different road roughnesses, which are $\boldsymbol{\Phi}_\mathbf{h}(\Omega_\mathbf{0}) = \mathbf{3}\,\boldsymbol{cm^3}$, $\boldsymbol{\Phi}_\mathbf{h}(\Omega_\mathbf{0}) = \mathbf{8}\,\boldsymbol{cm^3}$, $\boldsymbol{\Phi}_\mathbf{h}(\Omega_\mathbf{0}) = \mathbf{27}\,\boldsymbol{cm^3}$, and $\boldsymbol{\Phi}_\mathbf{h}(\Omega_\mathbf{0}) = \mathbf{60}\,\boldsymbol{cm^3}$. Note that the applied road roughnesses to the full-vehicle model are given in Table 3. Comfortable driving is proven with a value of $\mathbf{a_{w,rms}}$ less than 0.315 $\boldsymbol{m/s^2}$. When the value of $\mathbf{a_{w,rms}}$ exceeds $\mathbf{0.315}\,\boldsymbol{m/s^2}$, uncomfortable driving can be observed. For comfortable driving at selected road roughness, maximum school bus speeds are given in Table 5. The area above the region expressed by the dashed lines is an uncomfortable driving zone in Figure 3. To maintain comfortable driving, the vehicle speed should not exceed the values of $\mathbf{22.4}\,\boldsymbol{m/s}$, $\mathbf{12.8}\,\boldsymbol{m/s}$, $\mathbf{5.5}\,\boldsymbol{m/s}$ and $\mathbf{3.1}\,\boldsymbol{m/s}$ for $\boldsymbol{\Phi}_\mathbf{h}(\Omega_\mathbf{0}) = \mathbf{3}\,\boldsymbol{cm^3}$, $\boldsymbol{\Phi}_\mathbf{h}(\Omega_\mathbf{0}) = \mathbf{8}\,\boldsymbol{cm^3}$, $\boldsymbol{\Phi}_\mathbf{h}(\Omega_\mathbf{0}) = \mathbf{27}\,\boldsymbol{cm^3}$ and $\boldsymbol{\Phi}_\mathbf{h}(\Omega_\mathbf{0}) = \mathbf{60}\,\boldsymbol{cm^3}$ road roughnesses, respectively. For higher vehicle speeds than the calculated maximum speeds, uncomfortable driving will be inevitable, according to ISO 21631-1. The tolerance of the vehicle with $\boldsymbol{\Phi}_\mathbf{h}(\Omega_\mathbf{0}) = \mathbf{3}\,\boldsymbol{cm^3}$ is higher than that of others. It can be comfortable driving up to the PSD level of $\mathbf{22.4}\,\boldsymbol{m/s}$. As seen in Figure 3, driving on bad roads at high speeds causes uncomfortable driving. The selected PSDs of road roughness (A, B, C and D) are used as input for the full-vehicle model, and then maximum vehicle speeds are determined in terms of comfortable driving in Table 5. The driver should drive at very low speeds on D-class roads, otherwise, drivers may experience a high level of discomfort. If the maximum vehicle speed limit is exceeded, discomfort occurs, according to the 2631-1 Standard. Hence, if the limit is exceeded for a long time, health problems occur for the driver.

A general overview of the school bus model for road roughness and vehicle speed in terms of ISO 2631-1 is shown in Table 6 with color coding. If the frequency-weighted RMS accelerations of the bus seat vibrations that the driver is exposed to are higher than 0.315 $\boldsymbol{m/s^2}$, it is defined as uncomfortable driving. However, there are degrees of discomfort in this driving, depending on the acceleration values as given in Table 4. While the area below 0.315 $\boldsymbol{m/s^2}$ represents comfortable driving, exposure above 2 $\boldsymbol{m/s^2}$ represents an extremely uncomfortable driving zone. The frequency-weighted RMS acceleration values from the vehicle driver seat are evaluated in terms of driving comfort according to Table 4.

The cells of the table, which are filled in black, denote the cases where extremely uncomfortable driving is observed ($\mathbf{a_{w,rms}} > \mathbf{2}\,\boldsymbol{m/s^2}$). The grey, red, yellow, and blue cells in Table 6 represent very uncomfortable, uncomfortable, fairly uncomfortable, and a little uncomfortable driving, respectively. In addition, green areas represent comfortable driving. As seen in Table 6, uncomfortable driving conditions begin to appear as vehicle speed and the PSD of road roughness increase. Unhealthy driving zones are observed clearly in cases where PSDs of road roughness are very high ($\boldsymbol{\Phi}_\mathbf{h}(\Omega_\mathbf{0}) = \mathbf{323}\,\boldsymbol{cm^3}$ and $\boldsymbol{\Phi}_\mathbf{h}(\Omega_\mathbf{0}) = \mathbf{16300}\,\boldsymbol{cm^3}$). However, the condition of very low PSD of road roughness ($\boldsymbol{\Phi}_\mathbf{h}(\Omega_\mathbf{0}) = \mathbf{0.6}\,\boldsymbol{cm^3}$) is suitable for comfortable driving at all vehicle speeds. Thus, the effects of vehicle speed and road roughness on driving comfort are analyzed in detail.

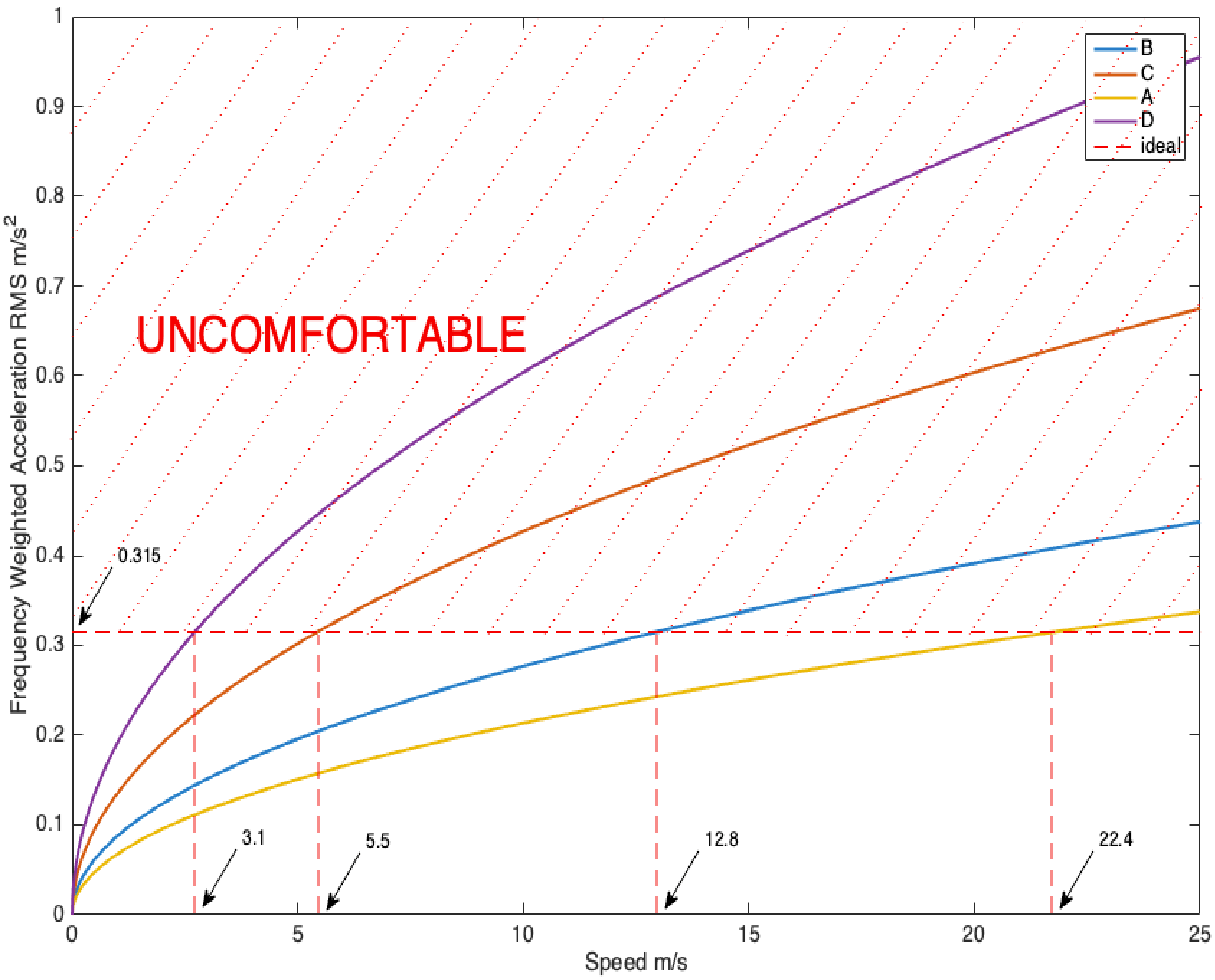

Figure 4. RMS acceleration vs vehicle speed for different road class.

Table 5. Maximum vehicle speeds based on different road types for comfortable driving.

Types of Roads	**PSD of Road Roughness ($\Phi_h(\Omega_0)cm^3$)**	**Maximum Vehicle Speeds (m/s)**
A	3	22.4
B	8	12.8
C	27	5.5
D	60	3.1

Table 6. The effects of road classes and vehicle speeds on driving comfort according to ISO 2631-1. (green) not uncomfortable driving, (blue) a little uncomfortable driving, (yellow) fairly uncomfortable driving, (red) uncomfortable driving, (grey) very uncomfortable driving, (black) extremely uncomfortable driving.

Road Class	Road Type	$\Phi_h(\Omega_0) cm^3$	Vehicle Speed (m/s) 1	3	5	7	9	11	13	15	17	19	21	23	25
Concrete	Very good	0.6													
	Good (A)	3													
	Medium	8.7													
	Bad	56													
Asphalt	Very good(B)	8													
	Good	11													
	Medium	22													
Cobblestone	Good	14													
	Medium (C)	27													
	Bad	36													
	Very bad	323													
Dirt	Good	32													
	Medium	44													
	Bad (D)	60													
	Very bad	16300													

3.2 Evaluation with Occupational Health and Safety Legislation

According to OHS regulations in Turkey, the evaluation of the vehicle speed and road roughness effects on bus driver health is observed in terms of bus seat vibrations in Table 7. Depending on this regulation, if the RMS accelerations of the bus seat vibrations that the driver is exposed to are higher than 0.5 m/s^2, it is defined as uncomfortable driving. Although frequency-weighted RMS accelerations of the bus seat vibrations are used as a comfort evaluation parameter for ISO 2631-1 evaluation, RMS accelerations of the bus seat vibrationsare used as an evaluation parameter in terms of bus driver health for OHS legislation evaluation. As seen in Table 7, the results evaluated with OHS regulations are different from the results evaluated with ISO 2631-1, especially at low PDS of road roughness. Healthy driving without precautions in terms of OHS regulations is observed in cases where PSDs of road roughness are low levels ($\Phi_h(\Omega_0) = 0.6\ cm^3$ and $\Phi_h(\Omega_0) = 3\ cm^3$, $\Phi_h(\Omega_0) = 8.7\ cm^3$ and $\Phi_h(\Omega_0) = 8\ cm^3$) for all vehicle speeds. However, the working conditions where measures should be taken by the employers arise in high road roughness ($\Phi_h(\Omega_0) = 323\ cm^3$ and $\Phi_h(\Omega_0) = 16300\ cm^3$) in accordance with OHS regulations.

Table 7. The effects of road classes and vehicle speeds on comfortable driving in accordance with OHS regulations. 🟦 comfortable driving, 🟥 uncomfortable driving.

Road Class	Road Type	$\Phi_h(\Omega_0)cm^3$	Vehicle Speed (m/s)												
			1	3	5	7	9	11	13	15	17	19	21	23	25
Concrete	Very good	0.6	🟦	🟦	🟦	🟦	🟦	🟦	🟦	🟦	🟦	🟦	🟦	🟦	🟦
	Good (A)	3	🟦	🟦	🟦	🟦	🟦	🟦	🟦	🟦	🟦	🟦	🟦	🟦	🟦
	Medium	8.7	🟦	🟦	🟦	🟦	🟦	🟦	🟦	🟦	🟦	🟦	🟦	🟦	🟦
	Bad	56	🟦	🟦	🟦	🟥	🟥	🟥	🟥	🟥	🟥	🟥	🟥	🟥	🟥
Asphalt	Very good(B)	8	🟦	🟦	🟦	🟦	🟦	🟦	🟦	🟦	🟦	🟦	🟦	🟦	🟦
	Good	11	🟦	🟦	🟦	🟦	🟦	🟦	🟦	🟦	🟦	🟦	🟦	🟥	🟥
	Medium	22	🟦	🟦	🟦	🟦	🟦	🟦	🟦	🟦	🟥	🟥	🟥	🟥	🟥
Cobblestone	Good	14	🟦	🟦	🟦	🟦	🟦	🟦	🟦	🟦	🟦	🟦	🟥	🟥	🟥
	Medium (C)	27	🟦	🟦	🟦	🟦	🟦	🟦	🟦	🟥	🟥	🟥	🟥	🟥	🟥
	Bad	36	🟦	🟦	🟦	🟦	🟦	🟥	🟥	🟥	🟥	🟥	🟥	🟥	🟥
	Very bad	323	🟥	🟥	🟥	🟥	🟥	🟥	🟥	🟥	🟥	🟥	🟥	🟥	🟥
Dirt	Good	32	🟦	🟦	🟦	🟦	🟦	🟦	🟥	🟥	🟥	🟥	🟥	🟥	🟥
	Medium	44	🟦	🟦	🟦	🟦	🟥	🟥	🟥	🟥	🟥	🟥	🟥	🟥	🟥
	Bad (D)	60	🟦	🟦	🟦	🟥	🟥	🟥	🟥	🟥	🟥	🟥	🟥	🟥	🟥
	Very bad	16300	🟥	🟥	🟥	🟥	🟥	🟥	🟥	🟥	🟥	🟥	🟥	🟥	🟥

4. Discussions

ISO 2631-1:1997 is an important standard for assessing the influences of whole-body vibration on driving comfort and human health. In this standard, procedures are proposed for assessing the influences of whole-body vibrations upon human health and driving comfort [25]. Standards are periodically revised to reflect advances in research and technology. Therefore, the specific requirements and criteria in each standard may change over time. BS 6841 is a British Standard with a focus on vertical whole-body vibrations and is primarily applicable in the UK, while ISO 2631-1 is an international standard that considers both vertical and horizontal vibrations and is widely recognized globally [26]. The choice of which standard to use may depend on regional regulations, industry practices, and the specific requirements of the assessment. The primary disparity discerned between BS 6841 and ISO 2631-1 lies in the distinct nature of the frequency weighting filters applied to vertical accelerations experienced on the seat cushion. Furthermore, in accordance with BS 6841:1987, it is suggested that the assessment of the impact of whole-body vibration on human health involves the consideration of the cumulative vibration resulting from three translational accelerations experienced on the seat cushion in conjunction with longitudinal accelerations experienced on the seat back. However, in ISO 2631-1:1997, it is recommended to take the highest value of the three translational accelerations on the seat cushion, or the vibration total value. The limits of the health guidance warning zone (HGCZ) in ISO 2631-1 are different from the EU Directive limits. The lower and upper limit values in ISO 2631-1, the EU 2002/44/EC directive, and the BS 6841 standard used in the assessment of whole-body vibration exposure differ in terms of vibration dose and vibration acceleration [27], [28]. When local regulations related to OHS are compared to all these standards, it is concluded that the regulations related to vibration are inadequate and limited in Turkey. While technical details, vibration dose calculations, and the effects of vibration on comfort are given in detail in other standards (ISO 2631-1, BS 6841, and EU), a general solution to vibration exposure is provided in the OHS local regulation in Turkey. This solution is quite inadequate in terms of the direction of vibration motion and calculations. While the classification of comfort criteria is detailed in the others, in the local OHS vibration regulation, which represents the local regulations, it is recommended to take the measures above $\mathbf{0.5}\, m/s^2$ and not exceed $\mathbf{1.15}\, m/s^2$ under any circumstances. This makes the regulation simple and less sensitive.

One of the innovative aspects of this study is the evaluation of vehicle seat vibrations using the local OHS vibration regulation and the comparison of these evaluations with ISO 2631-1. Also, the differences between the OHS regulation and other standards, as mentioned above, are discussed. The vibration exposures of school bus drivers at different road roughnesses and speeds are analyzed in terms of both ISO 2631-1 and OHS local regulations. As a result, it has been observed that ISO 2631-1 is more detailed and comprehensive in assessing the comfort status of school bus drivers.

The results from this study are compared with the seat vibration levels ($\mathbf{a_{w,rms}}$) reported in the literature for various road types and vehicle speeds in Table 8. The road types in our study were selected by estimating their correspondence to the road types in the literature. Subsequently, comparisons were made with the literature at equivalent speeds. This approach involved a thoughtful matching of road types from our study to those existing in the literature, followed by a thorough analysis and comparison of performance indicators, particularly at comparable speeds. This method ensured a systematic and meaningful alignment between our chosen road types and those identified in the literature, facilitating a comprehensive evaluation of the results within the established research context. It's observed that there are few differences between the study results and the findings of Lewis and Johnson, Blood et al., and Thamsuwan et al. [29]-[31]. The percentage error values highlight the extent of these differences. When this study is compared with the experimental studies in the literature, it is observed that the success of predicting $\mathbf{a_{w,rms}}$ values is high. It's important to note that variations may arise due to factors such as road conditions, asphalt quality, and the specific methodologies employed in different studies. The comparison provides valuable insights into the consistency and reliability of the study's vibration measurements across diverse road types and speeds.

Table 8. Comparison of the results of the study with the results of experimental studies in the literature.

Vehicle Speed (m/s)	Road types in literature	Road types in this study	This study results ($\mathbf{a_{w,rms}}$)	Lewis and Johnson results [29] ($\mathbf{a_{w,rms}}$)	Blood et. al. results [30] ($\mathbf{a_{w,rms}}$)	Thamsuwan et. al. results [31] ($\mathbf{a_{w,rms}}$)	Error (%)
23	Freeway	Medium Concrete	0.53	0.51	-	-	3.92
9	City Street	Medium Asphalt	0.42	0.47	-	-	10.63
8	City Street	Medium Asphalt	0.39	-	0.36	-	8.33
23	New freeway	Good Concrete	0.46	-	0.43	-	6.97
23	Old freeway	Bad Concrete	0.55	-	0.51	-	7.84
23.5	Smooth freeway	Good Concrete	0.47	-	-	0.42	11.89
26	Rough freeway	Bad Concrete	0.57	-	-	0.53	7.54
8.5	City street	Medium Asphalt	0.40	-	-	0.39	2.56

5. Conclusion and Suggestions

The eight-degrees-of-freedom vehicle model is developed to predict the maximum road roughness and vehicle speed for comfortable driving in terms of ISO 2631-1. This study is not performed with a real vehicle because the effect of changes in parameters cannot be clearly observed. Instead, the investigations are observed on the full-vehicle mathematical model. The analysis results in this study enabled us to consider the effects of different road roughness and vehicle speeds on frequency-weighted RMS accelerations of the seat, which are determined using weighted curves in the ISO 2631-1 Standard. Based on the observations from the study, the following conclusions in accordance with 2631-1 are reached:

- In order to be comfortable driving, it is concluded that the maximum vehicle speed increases as the PSD of road roughness decreases.
- The vehicle comfort problem can begin to feel as vehicle speed and PSD of road roughness rise.
- The vehicle speed range at which the vehicle can be driven comfortably is high at low PSDs.
- The maximum vehicle speed for comfortable driving increases as the value of PDS decreases.

The maximum vehicle speeds as a function of different road classes are determined in accordance with ISO 2631-1 and OHS legislation for comfortable driving. The comparison of OHS legislation and ISO 2631-1 evaluations is given in Table 8. Based on the comparisons, the following conclusions are reached:

- The driver's comfort is changed by the PSD of road roughness, regardless of evaluation methods.
- Safe and comfortable driving can be achieved with concrete roads. In order to feel comfortable driving on cobblestone roads, it is necessary to drive at low speeds.
- The maximum vehicle speed for comfortable driving decreases as road conditions worsen in both OHS legislation and ISO 2631-1 evaluations.
- For all road classes, OHS legislation offers a wider range of comfortable driving in terms of vehicle speed. For example, while uncomfortable driving begins to appear at $\mathbf{22.3}\ \boldsymbol{m/s}$ vehicle speed on a good asphalt road in accordance with OHS legislation, it occurs at $\mathbf{11.7}\ \boldsymbol{m/s}$ in accordance with ISO 2631-1.
- The health hazard is not observed on a very good concrete road in both OHS legislation and ISO 2631-1 evaluations.
- For all vehicle speeds, uncomfortable driving is inevitable on very bad dirt roads in both evaluation methods.
- Comfortable driving is suitable for all vehicle speeds on good concrete and medium concrete roads in accordance with OHS legislation. However, according to ISO 2631-1, uncomfortable driving occurs at higher speeds than 22.4 m/s and 11.7 m/s speeds ongood concrete and medium concrete roads, respectively.

The following precautions can be taken to reduce the effects of vibration on bus drivers in accordance with occupational health and safety:

- Minimizing travel distance
- Limiting vehicle speed
- Removing obstacles, filling potholes, and smoothing driving surfaces
- Providing a suitable suspension seat correctly adjusted for the driver's weight
- Equipping the driver seat with suspension
- Use of ergonomically designed seats and backrests that provide adequate padding
- Training school bus drivers for correct seat adjustment
- The school bus driver seat can be adjusted in various directions (up-down, front-back, right-left)

Contributions of the authors

Conceptualization, A.Y. and S.E.H.; methodology, A.Y.; validation, A.Y. and S.E.H.; formal analysis, A.Y.; investigation, A.Y. and S.E.H.; resources, A.Y.; data curation, A.Y. and S.E.H.; writing-original draft preparation, A.Y. and S.E.H.; writing-review and editing, A.Y. and S.E.H.; visualization, A.Y. and S.E.H. All authors have read and agreed to the published version of the manuscript.

Conflict of Interest Statement

There is no conflict of interest between the authors.

Table 9. Comparison of OHS legislation and ISO 2631-1 evaluations.

Road Class	Road Type	Maximum Vehicle Speed for Comfortable Driving (m/s)	
		OHS Legislation	**ISO 2631-1**
Concrete	Very good	-	-
	Good (A)	-	22.4
	Medium	-	11.7
	Bad	5.6	3.7
Asphalt	Very good (B)	-	12.8
	Good	22.3	11.7
	Medium	15.3	7.4
Cobblestone	Good	20.2	10.1
	Medium (C)	13.1	5.5
	Bad	9.7	3.7
	Very bad	0.2	0
Dirt	Good	11.7	5.2
	Medium	7.8	3.8
	Bad (D)	5.4	3.1
	Very bad	0	0

References

[1] M. Kolich and S. M. Taboun, “Ergonomics modelling and evaluation of automobile seat comfort,” *Ergonomics*, vol. 47, no. 8, pp. 841-863, 2004.

[2] A. Yavuz and A. Guney, “Optimization of Suspension Characteristics for Increasing Expected Daily Exposure Durations in Vehicles According to ISO 2631-1 Standard using Genetic Algorithms,” *INTER-NOISE and NOISE-CON Congress and Conference Proceedings*, vol. 259, pp. 6225–6234, 2019.

[3] N. Gültekin, M. Mayda, and M. Kilit, “Benzin ve Dizel Motorlarda Devir Sayısının Titreşime Olan Etkisinin İncelenmesi/Investigation of the Effect of Revolution of Diesel and Gasoline Engines on Their Vibration,” *Bitlis Eren Üniversitesi Fen Bilimleri Dergisi*, vol. 6, no. 2, pp. 39–43, 2017.

[4] S. E. Hacibektasoglu, B. Mertoglu, and H. Tozan, “Application of a novel hybrid f-SC risk analysis method in the paint industry,” *Sustainability*, vol. 13, no. 24, p. 13605, 2021.

[5] I. Morag and G. Luria, “A framework for performing workplace hazard and risk analysis: a participative ergonomics approach,” *Ergonomics*, vol. 56, no. 7, pp. 1086–1100, 2013.

[6] J. Wang, S. Han, and X. Li, “3D fuzzy ergonomic analysis for rapid workplace design and modification in construction,” *Autom. Constr.*, vol. 123, no. 103521, p. 103521, 2021.

[7] P. K. Marhavilas, D. Koulouriotis, and V. Gemeni, “Risk analysis and assessment methodologies in the work sites: On a review, classification and comparative study of the scientific literature of the period 2000–2009,” *J. Loss Prev. Process Ind.*, vol. 24, no. 5, pp. 477–523, 2011.

[8] *Çalışanların Titreşimle İlgili Risklerden Korunmalarına Dair Yönetmelik, Official Gazette 28743*. 2013.

[9] R. M. Lorente-Pedreille, F. Brocal, M. A. Saenz-Nuño, and M. A. Sebastián, “Analysis of metrological requirements in occupational health and safety regulations related to the emerging risk of exposure to vibrations,” *Appl. Sci. (Basel)*, vol. 10, no. 21, p. 7765, 2020.

[10] M. Bovenzi, "Low back pain disorders and exposure to whole-body vibration in the workplace," *Semin. Perinatol.*, vol. 20, no. 1, pp. 38–53, 1996.

[11] M. Milosevic and K. M. V. McConville, "Evaluation of protective gloves and working techniques for reducing hand-arm vibration exposure in the workplace," *J. Occup. Health*, vol. 54, no. 3, pp. 250–253, 2012.

[12] I. J. Tiemessen, C. T. J. Hulshof, and M. H. W. Frings-Dresen, "An overview of strategies to reduce whole-body vibration exposure on drivers: A systematic review," *Int. J. Ind. Ergon.*, vol. 37, no. 3, pp. 245–256, 2007.

[13] A. Guney, "Taşıtlarda Titreşim ve Gürültü," Lecture Notes, İTÜ, İstanbul, pp. 3-10, 1992.

[14] T. D. Gillespie, "Heavy Truck Ride," *in SAE Technical Paper Series*, 1985.

[15] P. Múčka, "Simulated road profiles according to ISO 8608 in vibration analysis". *Journal of Testing and Evaluation, vol.* 46, no. 1, pp. 405-418, 2017.

[16] P. Múčka, "Relation Between Seated Person Vibrations and the International Roughness Index" *Transportation Research Record*, vol. 2677, no. 6, pp. 351-364, 2023.

[17] P. Múčka, "New Transverse Unevenness Indexes of the Road Profile" *Journal of Transportation Engineering, Part B: Pavements*, vol. 148, no. 3, pp. 04022046, 2022.

[18] P. Múčka, G. J. Stein, P. Tobolka, "Whole-body vibration and vertical road profile displacement power spectral density" *Vehicle System Dynamics*, vol. 58, no. 4, pp. 630-656, 2020.

[19] İ. Karen, N. Kaya, F. Öztürk, İ. Korkmaz, M. Yıldızhan, and A. Yurttaş, "A design tool to evaluate the vehicle ride comfort characteristics: modeling, physical testing, and analysis," *Int. J. Adv. Manuf. Technol.*, vol. 60, no. 5–8, pp. 755–763, 2012.

[20] D. Sekulic, V. Dedovic, "The Effect of Stiffness and Damping of the Suspension System Elements on the Optimızation of the Vibratıonal Behaviour of a Bus," *International Journal for Traffic and Transport Engineering*, vol. 1, no. 4, pp. 231–244, 2011.

[21] H. Braun, T. Hellenbroich, "Messergebnisse von Straßenunebenheiten", VDI- Berichte Nr. 877, Düsseldorf: VDI-Verlag, 47-80, 1991.

[22] Mechanical Vibration and Shock-Evaluation of Human Exposure to Whole Body Vibration Part 1: General Requirements, International Organization for Standardization. Switzerland, 1997.

[23] M. Mitschke, Dynamik der Kraftfahrzeuge. Berlin: Springer-Verlag, 1984.

[24] MathWorks, Inc., *Student Edition of MATLAB Version 4: Student User Guide*. London, England: Prentice-Hall, 1995.

[25] P. Múčka, "Road roughness limit values based on measured vehicle vibration" *Journal of Infrastructure Systems*, vol. 23, no. 2, pp. 04016029, 2017.

[26] *Measurement and Evaluation of Human Exposure to Whole-Body Mechanical Vibration and Repeated Shock.* British Standards Institution, BS 6841, 1987.

[27] *Directive 2002/24/EC of the European Parliament and of the Council.* Official Journal of the European Communities, 2002.

[28] *T. Doğan, B. Erdem, Z. Duran, "Oturma Pozisyonunda Çalışanların Tüm Vücut Titreşimi Maruziyetlerinin Belirlenmesinde Kullanılan ISO2631-1, ISO2631-5, BS6841 ve Avrupa Birliği Direktifi (EU) 2002/44/EC'nin Karşılaştırılması" Ergonomi*, vol. 3, no. 2, pp. 108-117, 2020.

[29] *C.A. Le*wis, P.W. Johnson, "Whole-body vibration exposure in metropolitan bus drivers" *Occupational medicine*, vol. 62, no. 7, pp. 519-524, 2012.

[30] R.P. Blood, J.D. Ploger, M.G. Yost, R.P. Ching, P.W. Johnson, "Whole body vibration exposures in metropolitan bus drivers: A comparison of three seats" *Journal of Sound and Vibration*, vol. 329, no. 1, pp. 109-120, 2010.

[31] O. Thamsuwan, R.P. Blood, R.P. Ching, L. Boyle, P.W. Johnson, "Whole body vibration exposures in bus drivers: A comparison between a high-floor coach and a low-floor city bus" *International Journal of Industrial Ergonomics*, vol. 43, no. 1, pp. 9-17, 2013.